ELSEVIER

Carbaborane-functionalised 2,2′:6′,2″-terpyridine ligands for metallosupramolecular chemistry: Syntheses, complex formation, and the crystal and molecular structures of 4′-(*ortho*-carboranyl)-2,2′:6′,2″-terpyridine and 4′-(*ortho*-carboranylpropoxy)-2,2′:6′,2″-terpyridine [1]

Dominique Armspach, Edwin C. Constable *, Catherine E. Housecroft *, Markus Neuburger, Margareta Zehnder

Institut für Anorganische Chemie der Universität Basel, Spitalstrasse 51, CH-4056 Basel, Switzerland

Abstract

A series of functionalised 2,2′:6′,2″-terpyridine ligands, each with a *closo*-1,2-$C_2B_{10}H_{10}R$ (R = H or Si^tBuMe_2) substituent in the 4′ position, either directly or indirectly attached to the heterocyclic ring, has been prepared; two members of the series, 4′-(3-*ortho*-carboranylpropoxy)-2,2′:6′,2″-terpyridine (**4**) and 4′-(*ortho*-carboranyl)-2,2′:6′,2″-terpyridine (**7**) have been characterised by X-ray crystallography. The reaction of ligand (**7**) with alcohols results in the boron decapping of the *closo*-cage and yields a Zwitter-ionic *nido*-cluster-functionalised ligand. Analogous changes to the carbaborane cage have been observed in complexes in which the terpyridine domain is coordinated to ruthenium(II). However, decapping does not occur if a Si^tBuMe_2-protected carbaborane cage is incorporated into the terpyridine ligands. © 1998 Elsevier Science S.A.

1. Introduction

Metallosupramolecular chemistry is concerned with the use of metal centres to control assembly processes and/or as functional components of supramolecular systems [1]. We have recently been extending our studies of metal-based assemblies to the assembly of multinuclear dendritic systems [2–7]. In parallel we have been developing strategies for the introduction of clusters as functional groups onto such units [3,8–10] and have also developed the use of metal-assembled cores as structural units bearing molecular recognition [11] sites with a view to targeting specific biomolecular targets. We hope to use these various structural motifs for the specific targeting of biological sites with dendritic systems bearing multiple carbaborane functionalities. In this paper we describe in detail some of our preliminary studies in ligand design and report initial studies of the metallosupramolecular chemistry of the new carbaboranyl-functionalised ligands.

2. Experimental section

2.1. General data

Standard Schlenk and vacuum line techniques were used for all manipulation of air- and moisture-sensitive compounds. Reaction solvents were reagent grade and were distilled from appropriate drying agents under nitrogen before use. Benzene, THF and diethyl ether were distilled from sodium benzophenone ketyl; MeCN was distilled from P_4O_{10}. $B_{10}H_{14}$ (Dexsil) and 1,2-$C_2B_{10}H_{12}$ (Strem) were used as received. 4′-Hydroxy-2,2′:6′,6″-terpyridine [12], 4′-chloro-2,2′:6′,6″-terpyridine [12], [Ru(tpy)Cl$_3$] [13] and 1-(Si^tBuMe_2)-1,2-$C_2B_{10}H_{11}$ [14] were prepared according to literature methods.

---

* Corresponding authors. Fax: +41 061 267 1014. E-mail: housecroft@ubaclu.unibas.ch and constable@ubaclu.unibas.ch
[1] This paper is dedicated to Professor Ken Wade on the occasion of his 65th birthday.

^{1}H, ^{13}C and ^{11}B NMR spectra were recorded on Brüker AC 250 or Varian Gemini 300 spectrometers; for ^{11}B, $\delta = 0$ for $BF_3 \cdot Et_2O$. IR spectra were recorded on a ATI Mattson Genesis Series FTIR spectrometer. Positive-ion fast atom bombardment (FAB) mass spectra were recorded on a VG ZAB 2SEQ instrument, with 4-nitrobenzyl alcohol as matrix, and MALDI–TOF–MS measurements used a PerSeptive Biosystems Vestec spectrometer in positive linear mode at 5 kV acceleration voltage either without matrix or with a 2,5-dihydroxybenzoic acid matrix. Electrochemical measurements were performed with an Eco Chemie Autolab PGSTAT 20 potentiostat. A conventional three-electrode configuration was used, with glassy carbon working and platinum bead auxiliary electrodes and Ag/AgCl reference. For the electrochemical measurements, the solvent was freshly distilled acetonitrile. The base electrolyte was 0.1 M [^{n}Bu$_4$N][PF$_6$], recrystallised twice from ethanol/water and dried in vacuo over P_4O_{10}. Potentials are quoted vs. the Fc/Fc$^+$ couple, and all potentials were referenced to internal ferrocene added at the end of each experiment. All elemental analyses were performed by the Ciba Forschungsdienste Zentrale Analytik.

2.1.1. Preparation of 4′-(2-propyn-1-oxy)-2,2′:6′,6″-terpyridine (1)

A stirred solution of 4′-hydroxy-2,2′:6′,6″-terpyridine (HOtpy) (0.15 g, 0.60 mmol) in acetonitrile (20 ml) was treated with potassium carbonate (0.50 g, 3.62 mmol), followed by 3-bromoprop-1-yne (0.08 g, 0.67 mmol). The suspension was heated at 60°C under nitrogen for 12 h. After cooling to room temperature, the product was precipitated by pouring the reaction mixture into deionised water (100 ml). The solid precipitate was collected by filtration, washed with deionised water, dried in vacuo, and recrystallised from heptane to give (1) (95 mg, 55%) as colourless fine needles, m.p. 142–142.5°C. IR (KBr, cm^{-1}): 3257 (s), 3095 (w), 2113 (w), 1563 (s), 1584 (s), 1406 (m), 1196 (m), 1032 (s), 787 (m), 725 (m). ^{1}H NMR (CDCl$_3$): δ 2.55 (t, $^4J = 2.4$ Hz, 1H, $\equiv$CH), 4.91 (d, $^4J = 2.4$ Hz, 2H, CH$_2$), 7.30 (ddd, 2H, H^5), 7.81 (dt, 2H, H^4), 8.06 (s, 2H, H$^{3'}$), 8.58 (d, 2H, H^3), 8.66 (dd, 2H, H^6). ^{13}C NMR (CDCl$_3$): δ 55.8, 76.3, 77.6, 107.6, 121.3, 123.9, 136.7, 149.1, 155.9, 157.3, 165.8. MS (FAB): m/z 288 [M + H]$^+$, 250 [M-(HC$\equiv$CCH$_2$)]$^+$. Elem. anal.: Calc. for $C_{18}H_{13}N_3O$: C 75.25%, H 4.56%, N 14.62%; Found: C 74.99%, H 4.70%, N 14.59%.

2.1.2. Preparation of (2)

A solution of $B_{10}H_{14}$ (98 mg, 0.79 mmol) in anhydrous acetonitrile (5 ml) was refluxed under argon for 2 h and then the solvent was removed by distillation. The yellow residue was suspended in dry toluene (5 ml) and compound (1) (230 mg, 0.80 mmol) was added; the mixture was heated at reflux for 12 h and then evaporated to dryness. The residue was dissolved in CH_2Cl_2 (100 ml) and the solution filtered through celite. The organic layer was washed with water (50 ml), dried over Na_2SO_4, and filtered. The filtrate was evaporated to dryness to give a yellow–orange oil. After chromatographic separation [SiO_2, $CHCl_3$-MeOH–NH$_4$OH-(93:6:1)], the main fraction was collected and the solvent removed to yield (2) as an orange oil (16 mg, 5%). The compound was only partially characterised. ^{1}H NMR (CDCl$_3$): δ 4.12 (br, s, 1H, C$_{carb}$H), 4.64 (s, 2H, CH$_2$), 7.33 (ddd, 2H, H^5), 7.84 (dt, 2H, H^4), 7.95 (s, 2H, H$^{3'}$), 8.59 (dd, 2H, H^3), 8.67 (dd, 2H, H^6); ^{13}C NMR (CDCl$_3$): δ 58.0, 68.8, 105.9, 121.4, 124.3, 137.0, 149.1, 155.4, 157.6, 174.1.

2.1.3. Preparation of (3)

A solution of $B_{10}H_{14}$ (2.0 g, 16.4 mmol) in anhydrous acetonitrile (25 ml) was refluxed under argon for 2 h and then the solvent was removed by distillation. The yellow residue was suspended in dry toluene (25 ml) and 5-chloropent-1-yne (2.40 g, 23.4 mmol) was added. The reaction mixture was heated at reflux for 12 h. Evaporation of the solvent gave a yellow oily residue which was redissolved in CH_2Cl_2 and extracted with deionised water. The organic phase was then dried over $MgSO_4$ before being evaporated to dryness in vacuo. Column chromatographic separation [SiO_2, hexane–CH_2Cl_2 (4:2)], and removal of solvent afforded a colourless solid (2.1 g) which was dissolved in dry acetone (20 ml). Sodium iodide (1.40 g, 9.33 mmol) was added to the solution and the reaction mixture was heated at reflux for 12 h. After cooling to room temperature, solid NaCl was removed by filtration, and the filtrate was evaporated to dryness. Recrystallisation of the residue from heptane gave (3) (2.7 g, 53%) as a colourless solid, m.p. 55.5–56°C. IR (KBr, cm^{-1}): 3056 (m), 2959 (w), 2566 (s), 2360 (w), 2343 (w), 1450 (m), 1423 (w), 1291 (w), 1240 (w), 1173 (s), 1071 (m), 1016 (m), 720 (s), 612 (w), 504 (w). ^{1}H NMR (CDCl$_3$): δ 1.1–3.3 (br m, 10H, BH); 1.95 (m, 2H, CH$_2$CH$_2$CH$_2$), 2.30 (t, 2H, CH$_2$carb), 3.10 (t, 2H, CH$_2$I), 3.55 (br s, 1H, C$_{carb}$H); ^{13}C NMR (CDCl$_3$): δ 3.65, 32.34, 38.87, 61.52, 74.10; ^{11}B NMR (CDCl$_3$): δ −2.3 (d, 1B), −5.7 (d, 1B), −9.3 (d, 2B), −11.8 (d, 2B), −12.2 (d, 2B), −13.1 (d, 2B). MS (EI): m/z 311 [M]$^+$, 183 [M–I]$^+$. Elem. anal.: Calc. for $C_5H_{17}B_{10}I$: C 19.24%, H 5.49%; found C 19.40%, H 5.71%.

2.1.4. Preparation of compound (4)

A stirred solution of HOtpy (0.50 g, 2.01 mmol) in acetonitrile (10 ml) was treated with potassium carbonate (1.48 g, 10.7 mmol), followed by (3) (627 mg, 2.01 mmol). The suspension was heated at 60°C under nitrogen for 12 h and was then filtered through celite. The filtrate was evaporated to dryness in vacuo to give a

white residue which was subjected to column chromatography [SiO_2, CH_2Cl_2–MeOH–concentrated aqueous NH_3 solution (88:11:1)] to afford (**4**) (50 mg, 6%) as colourless crystals after recrystallisation from CH_2Cl_2–pentane, m.p.: 179–180°C. IR (KBr, cm^{-1}): 3042 (w), 2936 (w), 2588 (s), 1561 (s), 1466 (w), 1441 (w), 1404 (w), 1385 (w), 1354 (s), 1198 (m), 1056 (m), 991 (w), 794 (s), 745 (w), 620 (w). ^{1}H NMR ($CDCl_3$): δ 1.2–3.2 (br m, 10H, BH); 1.99 (m, 2H, $CH_2CH_2CH_2$), 2.42 (m, 2H, CH_2carb), 3.61 (br s, 1H, $C_{carb}H$); 4.17 (t, 2H, CH_2I), 7.30 (ddd, 2H, H^5), 7.83 (dt, 2H, H^4), 7.94 (s, 2H, $H^{3'}$), 8.59 (d, 2H, H^3), 8.65 (d, 2H, H^6). ^{13}C NMR ($CDCl_3$): δ 28.85, 34.96, 61.60, 66.32, 74.55, 107.10, 121.34, 123.96, 136.86, 149.03, 155.86, 157.23, 166.62. ^{11}B NMR ($CDCl_3$): δ −2.2 (d, 1B), −5.7 (d, 1B), −9.2 (d, 2B), −11.8 (d, 4B), −13.0 (d, 2B). MS (FAB): m/z 434 $[M + H]^+$. Elem. anal.: Calc. for $C_{20}H_{27}B_{10}N_3O$: C 55.41%, H 6.28%, N 9.69%; Found: C 55.04%, H 6.34%, N 9.66%.

2.1.5. Preparation of $[Ru(\mathbf{1})_2][PF_6]_2$

A stirred solution of $[Ru(HOtpy)_2][PF_6]_2$ (0.10 g, 0.11 mmol) in acetonitrile (20 ml) was treated with potassium carbonate (0.40 g, 2.90 mmol), followed by 3-bromoprop-1-yne (54 mg, 0.45 mmol). The suspension was heated at 60°C under nitrogen for 12 h and then filtered through celite. Water (10 ml) and a saturated methanolic $[NH_4][PF_6]$ solution (5 ml) were added to the filtrate. Partial removal of the solvents in vacuo caused $[Ru(\mathbf{1})_2][PF_6]_2$ to precipitate. The product was collected by filtration, washed with a mixture of water and ethanol, followed by diethyl ether, and dried in vacuo to afford pure $[Ru(\mathbf{1})_2][PF_6]_2$ (89 mg, 82%). IR (KBr, cm^{-1}): 3283 (w), 2361 (w), 2342 (w), 1612 (s), 1468 (m), 1415 (m), 1382 (w), 1354 (w), 1210 (s), 1009 (w), 837 (s), 787 (m), 558 (m). ^{1}H NMR (CD_3CN): δ 3.12 (t, $^4J = 2.4$ Hz, 2H, $\equiv$CH); 5.27 (d, $^4J = 2.4$ Hz, 4H, CH_2), 7.17 (m, 4H, H^5), 7.35 (d, 4H, H^6), 7.90 (dt, 4H, H^4), 8.37 (s, 4H, $H^{3'}$), 8.46 (d, 4H, H^3). ^{13}C NMR (CD_3CN): δ 58.63, 79.06, 103.54, 112.13, 125.39, 128.51, 138.83, 153.58, 157.52, 159.09, 165.53. MS (FAB): m/z 821 $[M-(PF_6)]^+$, 676 $[M-2(PF_6)]^+$, 637 $[M-2(PF_6)-(HC\equiv CCH_2)]^+$, 598 $[M-2(PF_6)-2(HC\equiv CCH_2)]^+$. Elem. anal.: Calc. for $C_{36}H_{26}F_{12}N_6O_2P_2Ru$: C 44.78%, H 2.71%, N 8.70%; Found: C 44.18%, H 3.04%, N 8.04%.

2.1.6. Preparation of $[Ru(\mathbf{2})_2][PF_6]_2$ and $[Ru(\mathbf{2})(tpy-OH)][PF_6]_2$

A solution of $B_{10}H_{14}$ (15 mg, 0.12 mmol) in anhydrous acetonitrile (2 ml) was refluxed under argon for 2 h after which $[Ru(\mathbf{1})_2][PF_6]_2$ (50 mg, 0.05 mmol) was added. The reaction mixture was then heated at reflux for 12 h. Removal of the solvent in vacuo gave a red solid. The products were separated by column chromatography [SiO_2, acetonitrile–saturated aqueous potassium nitrate solution (9:1)]; in order of their elution and after ion exchange: $[Ru(\mathbf{2})_2][PF_6]_2$ (17 mg, 27%), $[Ru(\mathbf{2})(HOtpy)][PF_6]_2$ (25 mg, 41%), and $[Ru(HOtpy)_2][PF_6]_2$ (3 mg, 6%) [13] were obtained.

$[Ru(\mathbf{2})_2][PF_6]_2$: IR (KBr, cm^{-1}): 3048 (w), 2579 (m), 2362 (w), 2344 (w), 1616 (s), 1467 (w), 1420 (w), 1395 (w), 1356 (s), 1211 (m), 1059 (w), 1025 (w), 846 (s), 787 (w), 558 (m), 442 (w). ^{1}H NMR (CD_3CN): δ 4.70 (br s, 2H, $C_{carb}H$), 5.04 (s, 4H, CH_2), 7.16 (ddd, 4H, H^5), 7.33 (d, 4H, H^6), 7.91 (dt, 4H, H^4), 8.32 (s, 4H, $H^{3'}$), 8.43 (d, 4H, H^3). ^{13}C NMR (CD_3CN): δ 61.80, 71.31, 98.08, 112.10, 125.38, 128.57, 138.91, 153.53, 157.57, 158.91, 165.34. ^{11}B NMR (CD_3CN): δ −2.5 (d, 2B), −4.0 (d, 2B), −8.9 (d, 4B), −11.1 (d, 8B), −12.5 (d, 4B). MS (FAB): m/z 1057 $[M-(PF_6)]^+$, 911 $[M-2(PF_6)]^+$, 755 $[M-2(PF_6)-(CH_2C_2B_{10}H_{11})]^+$, 598 $[M-2(PF_6)-2(CH_2C_2B_{10}H_{11})]^+$. Elem. anal.: Calc. for $C_{36}H_{46}B_{20}F_{12}N_6O_2P_2Ru$: C 35.97%, H 3.86%, N 6.99%; Found: C 35.00%, H 4.09%, N 7.01%.

$[Ru(\mathbf{2})(HOtpy)][PF_6]_2$: ^{1}H NMR ($CD_3CN$; see Fig. 1): δ 4.70 (br s, 1H, $C_{carb}H$), 5.04 (s, 2H, CH_2), 7.14 (m, 8H, H^{5A+5C}), 7.30 (d, 2H, H^{6C}), 7.43 (d, 2H, H^{6A}), 7.90 (m, 4H, H^{4A+4C}), 8.27 (s, 2H, $H^{3'B}$), 8.31 (s, 2H, $H^{3'D}$), 8.38 (d, 2H, H^{3A}), 8.42 (d, 2H, H^{3C}). MS (FAB): m/z 901 $[M-(PF_6)]^+$, 755 $[M-2(PF_6)]^+$, 598 $[M-2(PF_6)-(CH_2C_2B_{11})]^+$.

2.1.7. Preparation of $[Ru(\mathbf{4})_2][PF_6]_2$ and $[Ru(\mathbf{4})(\mathbf{5})][PF_6]$

A stirred solution of $[Ru(HOtpy)_2][PF_6]_2$ (0.20 g, 0.22 mmol) in acetonitrile (20 ml) was treated with potassium carbonate (0.20 g, 1.45 mmol), followed by (**3**) (155 mg, 0.50 mmol). The suspension was heated at 60°C under nitrogen for 24 h, and then filtered through celite. Water (10 ml) and saturated methanolic $[NH_4][PF_6]$ solution (5 ml) were added to the filtrate. Partial removal of the solvents in vacuo resulted in the precipitation of a red solid. After filtration, the solid residue was washed with a mixture of water and ethanol, then diethyl ether. The products were separated by TLC [SiO_2, acetonitrile–saturated aqueous potassium nitrate solution (7:1)] to afford in order of their elution, and after ion exchange: $[Ru(\mathbf{4})(\mathbf{5})][PF_6]$ (60 mg, 24%) and $[Ru(\mathbf{4})_2][PF_6]_2$ (85 mg, 30%); intractable material remained on the baseline.

$[Ru(\mathbf{4})(\mathbf{5})][PF_6]$: ^{1}H NMR ($CD_3CN$; see Fig. 1): δ 2.15–2.23 (m, 6H, overlapping $CH_2CH_2CH_2$ and -$CH_2(\mathbf{5})$), 2.66 (m, 2H, -$CH_2(\mathbf{4})$), 3.59 (br s, 1H, $C_{carb}H(\mathbf{5})$), 4.35 (br s, 1H, $C_{carb}H(\mathbf{4})$), 4.47 (t, $^3J = 6.1$ Hz, 2H, -$CH_2O(\mathbf{4})$), 4.53 (m, 2H, -$CH_2O(\mathbf{5})$), 7.15 (m, 4H, H^{5A+4C}), 7.35 (d, 2H, H^{6A}), 7.39 (d, 2H, H^{6C}), 7.88 (t, 4H, H^{4A+4C}), 8.25 (s, 2H, $H^{3'B}$), 8.34 (s, 2H, $H3'^D$), 8.44 (d, 2H, H^{3A}), 8.48 (d, 2H, H^{3C}). ^{11}B NMR (CD_3CN): δ −36.9 (d, 1B), −32.9 (d, 1B), −21.6 (d, 1B), −18.9 (d, 2B), −16.3 (d, 1B), −14.9 (d, 1B),
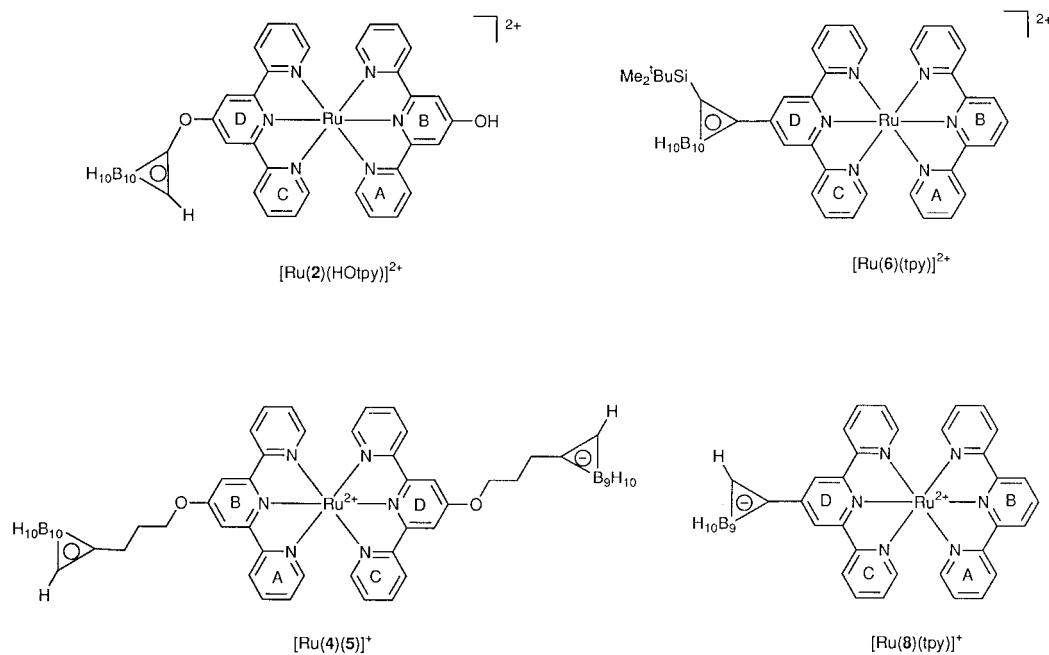
Fig. 1. The proposed structures of $[Ru(2)(HOtpy)]^{2+}$, $[Ru(5)(6)]^{+}$, $[Ru(6)(tpy)]^{2+}$ and $[Ru(8)(tpy)]^{+}$ and the ring nomenclature used for ^{1}H NMR spectroscopic assignments.

-12.7 (d, 2B), -11.6 (d, 4B), -12 to -10 [2] (d, 2B), -9.6 (d, 2B), -6.1 (d, 1B), -2.8 (d, 1B). MS (FAB): m/z 955 $[M-(PF_6)]^+$, 782 $[M-(PF_6)-((CH_2)_3C_2B_9H_{11})]^+$, 771 $[M-(PF_6)-((CH_2)_3C_2B_{10}H_{11})]^+$, 598 $[M-(PF_6)-((CH_2)_3C_2B_9H_{11})-((CH_2)_3C_2B_{10}H_{11})]^+$.

$[Ru(4)_2][PF_6]_2$: IR (KBr, cm^{-1}): 2924 (w), 2587 (m), 1614 (s), 1467 (w), 1422 (w), 1390 (w), 1356 (w), 1214 (m), 1059 (w), 1025 (w), 839 (s), 787 (w), 558 (m), 471 (w). ^{1}H NMR (CD$_3$CN): δ 2.15–2.23 (m, 4H, CH$_2$CH$_2$CH$_2$), 2.66 (m, 4H, -CH$_2$(4)), 4.35 (br s, 2H, C$_{carb}$H), 4.47 (t, 4H, -CH$_2$O), 7.13–7.17 (ddd, 4H, H^5), 7.36 (d, 4H, H^6), 7.88 (dt, 4H, H^4), 8.26 (s, 4H, H$^{3'}$), 8.45 (d, 4H, H^3). ^{13}C NMR (CD$_3$CN): δ 29.55, 34.74, 63.70, 69.50, 76.68, 111.87, 125.26, 128.37, 138.71, 153.45, 157.40, 159.20, 166.52. ^{11}B NMR (CD$_3$CN): δ -12.5 (d, 2B), -11.4 (d, 4B), -9.4 (d, 2B), -5.7 (d, 1B), -2.6 (d, 1B). MS (FAB): m/z 1113 [M-(PF$_6$)]$^+$, 967 [M-2(PF$_6$)]$^+$, 783 [M-(PF$_6$)-((CH$_2$)$_3$C$_2$B$_{10}$H$_{11}$)]$^+$, 598 [M-(PF$_6$)-2((CH$_2$)$_3$C$_2$B$_{10}$H$_{11}$)]$^+$. Elem. anal.: Calc. for C$_{40}$H$_{54}$B$_{20}$F$_{12}$N$_6$O$_2$P$_2$Ru: C 38.19%, H 4.33%, N 6.68%; Found: C 38.69%, H 4.34%, N 6.55%.

2.1.8. Preparation of (6)

A 1.6 M solution of ^{n}BuLi in hexanes (5.3 ml, 8.5 mmol) was added dropwise with stirring to a solution of 1-(Si^{t}BuMe$_2$)-1,2-C$_2$B$_{10}$H$_{11}$ (2.0 g, 7.7 mmol) in a dry

benzene/diethyl ether (2:1) mixture (25 ml) at 0°C. The mixture was stirred for 30 min while it warmed to room temperature. The solution was then cooled to 0°C and 4′-chloro-2,2′:6′,2″-terpyridine (Cltpy) in a solution of benzene/diethylether (2:1) mixture (100 ml) was added dropwise with stirring. After heating at reflux for 12 h, the solution was quenched with 100 ml of water, transferred to a separating funnel, and extracted with diethyl ether (3 × 50 ml). The combined organic phases were dried over anhydrous MgSO$_4$ before being evaporated to dryness. The yellow residue was filtered through a small plug of silica gel using CH$_2$Cl$_2$ as the eluant. Recrystallisation from heptane afforded compound (6) (2.15 g, 60%) as a colourless solid, m.p. 199.5–200°C. IR (KBr, cm^{-1}): 2928, 2577, 2361, 2342, 1582, 1464, 1384, 1088, 834, 822, 785. ^{1}H NMR (CDCl$_3$): δ -0.14 (s, 6H, SiMe$_2$); 0.88 (s, 9H, CMe$_3$); 1.2–3.8 (br m, 10H, BH); 7.33 (m, 2H, H^5); 7.83 (dt, 2H, H^4); 8.57 (d, 2H, H^3); 8.71 (br d, 2H, H^6); 8.76 (s, 2H, H$^{3'}$). ^{13}C NMR (CDCl$_3$): δ -3.76, 20.33, 27.19, 77.60, 83.25, 121.18, 122.86, 124.28, 136.83, 143.47, 149.40, 154.86, 156.03. ^{11}B NMR (CDCl$_3$): δ -11.8 (d, 2B); -9.2 (d, 2B); -7.2 (d, 4B); -2.4 (d, 1B); 1.9 (d, 1B). MS (FAB): m/z 491 $[M+H]^+$. Elem. anal.: calc. for C$_{23}$H$_{35}$B$_{10}$N$_3$Si: C 56.41%, H 7.20%, N 8.585; Found: C 55.90%, H 7.03%, N 8.32%.

2.1.9. Preparation of (7) by deprotection of (6)

A solution of (6) (1.88 g, 3.84 mmol) in dry THF (50 ml) was cooled to -78°C and a 1.0 M solution of dry [^{n}Bu$_4$N]F in THF (6 mmol in 6 ml) was added dropwise with stirring. The mixture was allowed to stir for

---

[2] Overlapping signals.

10 min while warming to room temperature, and then 20 ml of water were added. The solution was transferred to a separating funnel and extracted with diethyl ether (3×50 ml). The combined organic phases were dried over $MgSO_4$ and filtered. Removal of the solvent in vacuo gave a colourless residue which was subjected to flash chromatography [SiO_2, CH_2Cl_2–MeOH–concentrated aqueous NH_3 solution (90:9:1)], followed by recrystallisation from hexane to yield compound (**7**) as a colourless solid (0.8 g, 56%), m.p. 209.5–210°C. IR (KBr, cm^{-1}): 3061, 2993, 2856, 1582, 1565, 1466, 1395, 1266, 1080, 800, 785. ^{1}H NMR ($CDCl_3$): δ 4.30 (br s, 1H, $C_{carb}H$); 1.0–3.6 (br m, 10H, BH); 7.34 (m, 2H, H^5); 7.84 (dt, 2H, H^4); 8.52 (s, 2H, $H^{3'}$); 8.56 (d, 2H, H^3); 8.68 (br d, 2H, H^6). ^{13}C NMR ($CDCl_3$): δ 58.80, 74.50, 118.48, 121.42, 124.47, 137.02, 144.19, 149.28, 154.75, 156.38; ^{11}B NMR ($CDCl_3$): δ −12.8 (d, 2B); −11.1 (d, 4B); −8.7 (d, 2B), −3.6 (d, 1B), −2.1 (d, 1B). MS (FAB): m/z 376 $[M+H]^+$. Elem. anal.: Calc. for $C_{17}H_{21}B_{10}N_3$: C 54.38%, H 5.64%, N 11.19%; Found: C, 52.8%; H, 6.0%; N, 10.0%.

2.1.10. Preparation of [Fe(**6**)$_2$][PF$_6$]$_2$

A solution of (**6**) (100 mg, 0.20 mmol) in methanol (2 ml) was added to a solution of $[NH_4]_2Fe[SO_4]_2 \cdot 6H_2O$ (80 mg, 0.20 mmol) in methanol (3 ml). The mixture was stirred at room temperature for 10 min and then excess aqueous $[NH_4][PF_6]$ was added. The resulting precipitate was collected by filtration, washed with a small amount of ice-cold methanol, water, and diethyl ether, and dried in vacuo to yield [Fe(**6**)$_2$][PF$_6$]$_2$ as a purple solid (0.132 g, 97%). IR (KBr, cm^{-1}): 2935, 2576, 1609, 1426, 1074, 1031, 841, 785. ^{1}H NMR (CD_3CN): δ 0.19 (s, 12H, SiMe$_2$); 1.09 (s, 18 H, CMe$_3$); 1.3–3.8 (br m, 20 H, BH); 6.96 (br d, 4H, H^6), 7.12 (m, 4H, H^5); 7.93 (dt, 4H, H^4); 8.71 (br d, 4H, H^3); 8.98 (s, 4H, $H^{3'}$). ^{13}C NMR (CD_3CN): δ −2.95, 21.18, 27.30, 80.7, 82.2, 125.71, 126.29, 128.92, 140.02, 144.45, 153.70, 157.63, 161.68. ^{11}B NMR (CD_3CN): δ −11.3 (d, 4B); −8.4 (d, 4B); −6.0 (d, 8B); −1.5 (d, 2B); 2.6 (d, 2B); MS (MALDI–TOF): m/z 1036 $[M-2PF_6]^+$.

2.1.11. Preparation of [Ru(tpy)(**6**)][PF$_6$]$_2$

Compound (**6**) (111 mg, 0.23 mmol) was added to a suspension of [Ru(tpy)Cl$_3$] (100 mg, 0.23 mmol) in methanol (30 ml). Two drops of *N*-ethylmorpholine were added to the mixture which was then heated at reflux with stirring for 1 h. The resulting deep red solution was filtered through celite and excess aqueous $[NH_4][PF_6]$ was added to precipitate hexafluorophosphate salts, which were collected by filtration and washed with ice-cold methanol, water and diethyl ether. The red solid so obtained was subjected to column chromatography [SiO_2, acetonitrile–saturated aqueous potassium nitrate solution–water (23:2:1)]; treatment of

the main fraction with excess aqueous $[NH_4][PF_6]$ caused a red solid to precipitate. This was separated by filtration, washed with ice-cold methanol and the diethyl ether, and dried in vacuo to yield solid [Ru(tpy)(**6**)][PF$_6$]$_2$ (60 mg, 28%). IR (KBr, cm^{-1}): 2573, 1637, 1604, 1422, 1389, 840, 766, 537. ^{1}H NMR (CD_3CN; see Fig. 1): δ 0.12 (s, 6H, SiMe$_2$); 1.06 (s, 9H, CMe$_3$); 1.3–3.8 (br m, 10H, BH); 7.16 (m, 4H, H^{5A+5C}); 7.23 (m, 2H, H^{6C}); 7.39 (d, 2H, H^{6A}); 7.93 (t, 2H, H^{4A}); 7.96 (t, 2H, H^{4C}); 8.47 (t, 1H, H^{4B}); 8.50 (d, 2H, H^{4A}); 8.71 (d, 2H, H^{3B}); 8.78 (d, 2H, H^{3C}); 8.79 (s, 2H, H^{3D}). ^{13}C NMR (CD_3CN): δ −3.12, 21.12, 27.34, 80.82, 84.56, 124.91, 125.61, 125.74, 126.43, 128.35, 129.13, 137.60, 139. 05, 139.37, 141.08, 153.13, 153.53, 155.79, 156.97, 157.90, 158.76. ^{11}B NMR (CD_3CN): δ −11.1 (d, 2B); −8.4 (d, 2B), −6.2 (d, 4B); −2.4 (d, 1B); 2.6 (d, 1B). MS (MALDI–TOF): m/z 827 for $[M-PF_6^+]$.

2.1.12. Preparation of [Ru(**8**)$_2$]

A suspension of $RuCl_3 \cdot 3H_2O$ (105 mg, 0.40 mmol) in ethane-1,2-diol (10 ml) was stirred at room tempera-

Table 1
Fractional atomic coordinates for compound (**4**)

	x	y	z
C(1)	1.1336(1)	−0.1197(2)	0.01478(8)
C(2)	1.2240(1)	−0.1959(2)	0.00820(8)
C(3)	1.2249(1)	−0.3315(2)	0.02940(8)
C(4)	1.1356(1)	−0.3880(1)	0.05560(7)
C(5)	1.04775(9)	−0.3042(1)	0.05997(6)
N(1)	1.04638(9)	−0.1711(1)	0.04019(6)
C(6)	0.94883(9)	−0.3596(1)	0.08615(6)
C(7)	0.85822(9)	−0.2801(1)	0.08359(6)
C(8)	0.76667(9)	−0.3374(1)	0.10666(6)
C(9)	0.76741(8)	−0.4738(1)	0.13052(6)
C(10)	0.86284(8)	−0.5451(1)	0.13184(5)
N(2)	0.95182(7)	−0.49022(9)	0.11112(5)
C(11)	0.86902(8)	−0.6928(1)	0.15501(6)
C(12)	0.95911(9)	−0.7701(1)	0.14558(7)
C(13)	0.9604(1)	−0.9086(1)	0.16383(8)
C(14)	0.8729(1)	−0.9660(1)	0.19129(8)
C(15)	0.7883(1)	−0.8810(1)	0.20059(8)
N(3)	0.78416(8)	−0.7466(1)	0.18318(6)
O(1)	0.68191(7)	−0.25188(8)	0.10363(5)
C(16)	0.5831(1)	−0.3068(1)	0.12167(8)
C(17)	0.50387(9)	−0.1901(1)	0.11358(7)
C(18)	0.5258(1)	−0.0759(1)	0.16622(7)
C(19)	0.45488(8)	0.0514(1)	0.16148(6)
C(20)	0.38929(9)	0.0917(1)	0.23135(6)
B(1)	0.3217(1)	0.0278(1)	0.15891(8)
B(2)	0.3849(1)	0.1008(1)	0.08739(7)
B(3)	0.4926(1)	0.1999(2)	0.12165(8)
B(4)	0.4952(1)	0.1894(1)	0.21379(8)
B(5)	0.2723(1)	0.1655(2)	0.20938(8)
B(6)	0.2687(1)	0.1766(2)	0.11676(8)
B(7)	0.3746(1)	0.2838(2)	0.09352(8)
B(8)	0.4436(1)	0.3381(2)	0.17186(9)
B(9)	0.3802(1)	0.2656(2)	0.24322(7)
B(10)	0.3046(1)	0.3233(2)	0.16900(8)

ture for 30 min and then compound (**7**) (300 mg, 0.80 mmol) was added. The reaction mixture was heated to 120°C and this temperature maintained for 3 h with constant stirring. Upon cooling to room temperature, a suspension was obtained which was filtered; the solid obtained was washed sequentially with ethane-1,2-diol, water, methanol and diethyl ether to yield [Ru(**8**)$_2$] as a dark red solid (160 mg, 48%). IR (KBr, cm^{-1}): 2527, 1604, 1465, 1422, 1406, 1027, 786, 751. ^{1}H NMR (d_6-DMSO) δ 0.3–3.2 (br m, 20H, BH); 3.25 (br s, 2H, C$_{carb}$H); 7.22 (m, 4H, H^5); 7.31 (br d, 4H, H^6); 7.92 (dt, 4H, H^4); 8.61 (s, 4H, H$^{3'}$); 8.88 (br d, 4H, H^3). ^{13}C NMR (d_6-DMSO) δ 119.88, 124.15, 127.57, 137.72, 151.90, 153.18, 155.18, 157.83. ^{11}B NMR (d_6-DMSO) δ −3.40 (d, 2B); −7.5 (d, 2B); −9.2 (d, 2B); −12.2 (d, 2B); −15.3 (d, 2B); −19.1 (2 × d, 4B); −22.6 (d, 2B); −31.8 (d, 2B). MS (MALDI–TOF): m/z 831 [M$^+$].

2.1.13. Preparation of [Ru(tpy)(**8**)][PF$_6$]

Compound (**7**) (300 mg, 0.80 mmol) was added to a solution of [Ru(tpy)Cl$_3$] (352 mg, 0.80 mmol) in methanol (60 ml). Two drops of *N*-ethylmorpholine were added to the mixture which was subsequently stirred at reflux for 1 h. The resulting deep red solution was filtered through celite and excess aqueous [NH$_4$][PF$_6$] was added to precipitate the product as its hexafluorophosphate salt. After filtering, the residue was washed with ice-cold methanol, water, and then diethyl ether, and the red product mixture was separated by using column chromatography [SiO$_2$, acetonitrile–saturated aqueous potassium nitrate solution–water 47:2:1]. The major fraction was [Ru(tpy)(**8**)][PF$_6$], which was isolated as a dark red solid (140 mg, 21%). IR (KBr): 2529, 1606, 1465, 1448, 1423, 1385, 1029, 841, 767, 558. ^{1}H NMR (CD$_3$CN; see Fig. 1): δ 0.3–3.2 (br

m, 10H, BH); 2.89 (br s, 1H, C$_{carb}$H); 7.07 (ddd, 2H, H^{5C}); 7.16 (ddd, 2H, H^{5A}); 7.23 (br d, 2H, H^{6C}); 7.35 (br d, 2H, H^{6A}); 7.88 (2 × dt, 4H, H$^{4A + 4C}$); 8.34 (t, 1H, H$^{4'B}$); 8.44 (d, 2H, H^{3C}); 8.47 (s, 2H, H$^{3'D}$), 8.50 (d, 2H, H^{3A}); 8.70 (d, 2H, H$^{3'B}$). ^{13}C NMR (CD$_3$CN): δ 44.07, 117.89, 117.98, 121.75, 124.52, 135.22, 125.29, 128.08, 128.45, 136.23, 138.82, 153.39 (×2), 154.77, 156.60, 159.04, 159.35. ^{11}B NMR (CD$_3$CN): δ −7.4 (d, 1B); −9.2 (d, 1B); −12.5 (d, 1B); −15.9 (d, 1B); −16.8 (d, 1B); −19.1 (d, 1B); −22.2 (d, 1B); −31.9 (d, 1B); −34.5 (d, 1B). MS (MALDI–TOF): m/z 699 [M-PF$_6$]$^+$.

2.2. Crystal structure determination of (**4**) and (**7**)

2.2.1. Crystal data for (**4**)

C$_{20}$H$_{27}$B$_{10}$N$_3$O, colourless blocks, crystal size 0.35 × 0.50 × 0.80 mm, $M = 433.57$, monoclinic, space group $P2_1/n$, $a = 12.796(1)$, $b = 9.624(1)$, $c = 19.097(1)$ Å, $\beta = 92.687(6)$ Å, $V = 2349.2(3)$ Å^3, $F(000) = 906$, $Z = 4$, $D_c = 1.23$ g cm^{-3}, μ(Cu–Kα) $= 4.897$ cm^{-1}.

2.2.2. Crystal data for (**7**)

C$_{17}$H$_{21}$N$_3$B$_{10}$, colourless blocks, crystal size 0.38 × 0.54 × 0.58 mm, $M = 375.49$, triclinic, space group

Table 3
Fractional atomic coordinates for compound (**7**)

	x	y	z
N(1)	−0.7377(2)	−0.01948(9)	0.07142(9)
N(2)	−0.1975(1)	0.05263(9)	0.20948(8)
N(3)	0.3370(2)	0.21760(9)	0.35514(9)
C(1)	−0.9107(2)	−0.1137(1)	0.0320(1)
C(2)	−0.9149(2)	−0.2284(1)	0.0349(1)
C(3)	−0.7320(2)	−0.2466(1)	0.0778(1)
C(4)	−0.5508(2)	−0.1510(1)	0.1181(1)
C(5)	−0.5613(2)	−0.0379(1)	0.11468(9)
C(6)	−0.3739(2)	0.0707(1)	0.16618(9)
C(7)	−0.3900(2)	0.1867(1)	0.17415(9)
C(8)	−0.2172(2)	0.2873(1)	0.23259(9)
C(9)	−0.0333(2)	0.2691(1)	0.2780(1)
C(10)	−0.0294(2)	0.1496(1)	0.26349(9)
C(11)	0.1618(2)	0.1246(1)	0.31252(9)
C(12)	0.1550(2)	0.0084(1)	0.3135(1)
C(13)	0.3360(2)	−0.0114(1)	0.3594(1)
C(14)	0.5167(2)	0.0838(1)	0.4044(1)
C(15)	0.5086(2)	0.1962(1)	0.4008(1)
C(16)	−0.2318(2)	0.4155(1)	0.25229(9)
C(17)	−0.4429(2)	0.4416(1)	0.2779(1)
B(1)	−0.2177(2)	0.4998(1)	0.3815(1)
B(2)	−0.0250(2)	0.5436(1)	0.3236(1)
B(3)	−0.1448(2)	0.5034(1)	0.1851(1)
B(4)	−0.4142(2)	0.4346(1)	0.1564(1)
B(5)	−0.5154(2)	0.5444(1)	0.2293(1)
B(6)	−0.3953(2)	0.5845(1)	0.3675(1)
B(7)	−0.1261(2)	0.6537(1)	0.3961(1)
B(8)	−0.0811(2)	0.6566(1)	0.2749(1)
B(9)	−0.3224(2)	0.5890(1)	0.1714(1)
B(10)	−0.3098(2)	0.6823(1)	0.3018(1)

Table 2
Selected bond distances and angles for compound (**4**)

Bond distances (Å)			
C(5)–C(6)	1.482(2)	C(10)–C(11)	1.490(1)
C(19)–B(1)	1.718(2)	C(19)–B(2)	1.706(2)
C(19)–B(3)	1.700(2)	C(19)–B(4)	1.727(2)
C(20)–B(1)	1.711(2)	C(20)–B(4)	1.696(2)
C(20)–B(5)	1.692(2)	C(20)–B(9)	1.693(2)
C(19)–C(20)	1.655(1)	C(8)–O(1)	1.361(1)
O(1)–C(16)	1.428(1)	C(16)–C(17)	1.516(2)
C(17)–C(18)	1.507(2)	C(18)–C(19)	1.524(2)
Bond angles (°)			
C(18)–C(19)–C(20)	117.6(1)	C(18)–C(19)–B(1)	118.9(1)
C(18)–C(19)–B(2)	124.1(1)	C(18)–C(19)–B(3)	121.5(1)
C(18)–C(19)–B(4)	115.0(1)	C(17)–C(18)–C(19)	117.1(1)
C(16)–C(17)–C(18)	111.7(1)	O(1)–C(16)–C(17)	107.3(1)
C(8)–O(1)–C(16)	118.6(1)		
Dihedral angles (°)			
N(3)–C(11)–C(10)–N(2)	7.0		
N(2)–C(6)–C(5)–N(1)	4.9		

$P\bar{1}$, $a = 6.935(1)$, $b = 12.062(1)$, $c = 13.817(3)$ Å, $\alpha = 107.827(13)$, $\beta = 102.532(13)$, $\gamma = 102.222(8)$ Å, $V = 1024.9(3)$ Å^3, $F(000) = 388$, $Z = 2$, $D_c = 1.217$ g cm^{-3}, $\mu(\text{Cu–K}\alpha) = 4.54$ cm^{-1}.

2.2.3. Data collection and refinement for (4) and (7)

The crystals selected for X-ray structure determination were stuck with oil on to glass fibres. Unit cell parameters were determined by the least-squares method using 24 for (4) or 25 for (7) carefully centred independent reflections. Data collection was carried out at 298 K for (4) and 293 K for (7) on a four-circle Enraf-Nonius CAD4 diffractometer using monochromatised Cu–$K\alpha$ radiation ($\lambda = 1.54178$ Å). The $\omega - 2\theta$ technique was used to measure 5297 reflections for (4) and 4356 reflections for (7), both in the range $5° \leq 2\theta \leq 148°$. Three standard reflections monitored every hour during data collection showed no significant decay in either case. For (4), the 4167 unique data with $I \geq 3\sigma(I)$ were used to solve and refine the structure. The usual corrections were applied. The absorption correction was determined by ψ scans (max/min transmission 1.00/0.91). For (7), the 3871 unique data with $I \geq 3\sigma(I)$ were used to solve and refine the structure. The usual corrections were applied. The absorption correction was determined by ψ scans (max/min transmission 1.00/0.58).

2.2.4. Structural analysis and refinement

The structures were solved by direct methods using the program SIR92 [15]. Anisotropic least-squares refinement was carried out on all non-hydrogen atoms except those of the acetonitrile and water solvent molecules using the program CRYSTALS [16]. The hydrogen atoms are in calculated positions with a fixed distance of 1.0 Å. Scattering factors were taken from the International Tables for X-ray Crystallography [17]. For (4), the final R values were 0.043 and 0.051 and the final Fourier-difference maps were featureless. Atomic coordinates are given in Table 1 and selected

bond lengths and angles in Table 2. For (7), the final R values were 0.057 and 0.065 and the final Fourier-difference maps had min/max values of $-0.271/0.298$ e Å^{-3}. Atomic coordinates are given in Table 3 and selected bond lengths and angles in Table 4.

Atomic coordinates, thermal parameters and bond lengths and angles have been deposited at the Cambridge Crystallographic Data Centre.

3. Results and discussion

3.1. Ligand design and synthetic strategy

We decided to adopt the 2,2′:6′,2″-terpyridine (tpy) metal-binding domain as the basic ligand structure to which carbaboranyl substituents were to be appended. The reasons for the adoption of this domain have been described in detail elsewhere but are related to the stereogenic properties of the tpy domain when coordinated to six-coordinate metal centres [18,19]; in contrast to derivatised 2,2′-bipyridine ligands, 4′-substituted tpy ligands give neither optical nor *mer/fac* isomers with such metal centres. We also decided, in the first instance, to introduce functionality in the form of *closo–ortho*-carbaboranyl substituents. This decision was dictated by the stability and ready availability of the cluster core, together with the known and extensive organic chemistry of such carbaboranes [20,21].

This led us to consider a number of possible strategies, varying in the synthetic timing of the assembly of the carbaborane cluster unit. We proposed two possible strategies: (1) preparation of an alkyne-functionalised tpy ligand which would subsequently be reacted with $B_{10}H_{14}$ to generate the carbaborane in the final step, or (2) the preparation of a suitably functionalised carbaborane which would be coupled with the tpy domain in the final steps of the reaction sequence. In view of our previous use of the metal-directed reactivity of coordinated oligopyridine ligands in the synthesis of novel species [22–24], we also kept in mind the possibility of devising sub-strategies in which coordinated tpy ligands were the precursors. Both of the strategies allow considerable flexibility in the synthesis and permit the introduction of variable spacer groups between the tpy and the carbaboranyl domains.

3.2. Ligands with spacers between the tpy and carbaboranyl domains

We initially decided to adopt the metal-free strategy (1) for the synthesis of species with flexible spacers between the tpy and carbaboranyl domains and our entry involved the reaction between decaborane(14) and an alkynyl-substituted tpy ligand (Scheme 1). The de-

Table 4
Selected bond distances and angles for compound (7)

Bond distances (Å)

C(5)–C(6)	1.490(2)	C(10)–C(11)	1.488(2)
C(8)–C(16)	1.515(1)	C(16)–C(17)	1.649(1)
C(16)–B(1)	1.733(2)	C(16)–B(2)	1.712(2)
C(16)–B(3)	1.711(2)	C(16)–B(4)	1.730(2)

Bond angles (°)

C(8)–C(16)–C(17)	116.60(9)	C(8)–C(16)–B(1)	115.80(9)
C(8)–C(16)–B(2)	123.08(9)	C(8)–C(16)–B(3)	123.9(1)
C(8)–C(16)–B(4)	117.18(9)	C(9)–C(8)–C(16)	120.3(1)
C(7)–C(8)–C(16)	120.6(1)		

Dihedral angles (°)

N(3)–C(11)–C(10)–N(2)	8.2
N(2)–C(6)–C(5)–N(1)	0.0
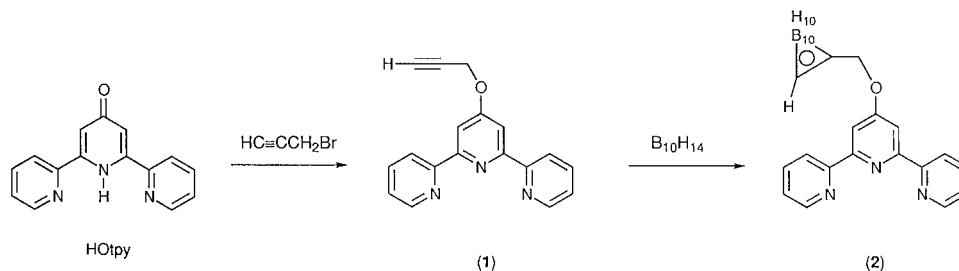
Scheme 1.

sired alkynyl functionalised tpy ligands could be conveniently prepared by alkylation of the oxygen atom of 2,2′:6′,2″-terpyridin-4′($1'H$)-one (HOtpy) [12]. In the first step of the sequence, HOtpy was reacted with 3-bromoprop-1-yne in the presence of base to give the alkynyl-substituted tpy (**1**) as a white crystalline solid in 56% yield. Compound (**1**) exhibited the expected spectroscopic properties and was subsequently reacted with $B_{10}H_{14}$ in acetonitrile. However, this reaction yielded the desired compound (**2**) in optimised yields of $\leq 5\%$. The low and unreproducible yield of (**2**) prevented its full characterisation and its identity is proposed on the basis of ^{1}H and ^{13}C NMR spectroscopies. The ^{1}H NMR spectrum of (**2**) showed typical signals for the tpy moiety and the coupling constants for the tpy unit in this and all other compounds were as previously reported [13]. The most diagnostic feature is the observation of $H^{3'}$, the proton directly next to the site of attachment of the substituent, at δ 7.95, in contrast to its chemical shift of δ 8.06 in the starting material (**1**). Mixtures of (**1**) and (**2**) clearly showed two separate singlets for the two $H^{3'}$ environments, eliminating the possibility of medium or concentration effects resulting in the shift. The metal-directed substrategy is discussed later.

Scheme 2 shows our second strategy, in which a functionalised C_2B_{10} cage bearing an electrophilic site, which could subsequently be reacted with HOtpy, was
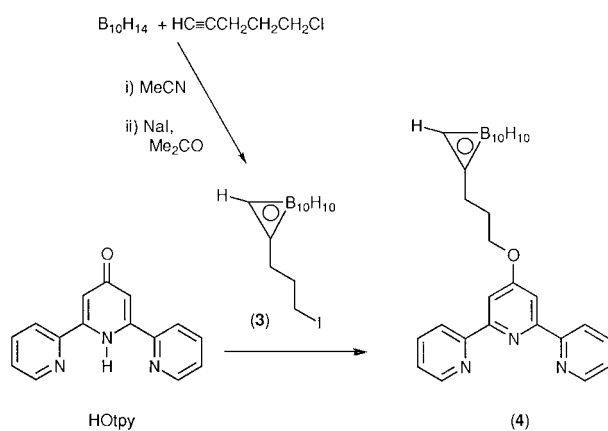
assembled before attachment to the heterocyclic ligand. Activation of decaborane by heating in acetonitrile followed by reaction with 5-chloropent-1-yne yielded an intermediate 1-(3-chloropropyl)-*closo*-1,2-carbaborane, which was isolated as a colourless oil but which was not further characterised. We considered that the pendant chloropropyl group would only be moderately electrophilic and decided to convert the crude chloropropyl compound directly to the 3-iodopropyl analogue (**3**) in a Finkelstein reaction with sodium iodide in acetone. After recrystallisation, the cluster derivative (**3**) was isolated in 53% yield as a white solid. Both the ^{11}B and ^{13}C NMR spectra of (**3**) were in accord with a *closo*-1-R-1,2-$C_2B_{10}H_{11}$ cluster and this was supported by mass spectroscopic data. In particular, the ^{11}B NMR spectrum exhibited six resonances in a 2:2:2:2:1:1 ratio in the δ −2 to −14 region and the electron impact mass spectrum showed the expected parent ion at m/z 311. The ^{1}H and ^{13}C NMR spectra of compound (**3**) were fully consistent with the presence of the 3-iodopropyl chain. Compound (**3**) reacted with HOtpy in the presence of potassium carbonate to yield the ether (**4**) as a white solid. Spectroscopic and mass spectrometric data were consistent with the formulation of (**4**). The most important features were the observation of resonances similar to those for (**3**) in the ^{11}B NMR spectrum, the appearance of a new $H^{3'}$ peak at δ 7.94 in the ^{1}H NMR spectrum and the correct partial microanalysis. All of these suggested that the *closo*-1,2-$C_2B_{10}H_{11}$-unit had remained intact in the reaction sequence and this was confirmed by the results of an X-ray crystallographic study.

Single crystals of compound (**4**) suitable for X-ray diffraction were grown from chloroform. The molecular structure of (**4**) is shown in Fig. 2 and selected bond distances and angles are listed in Table 2. The structural determination confirms the gross structural features of the molecule. The structural parameters for the ordered *closo*-C_2B_{10} cage are unexceptional [25]; the C(19)–C(20) edge is 1.655(1) Å. The propoxy-chain is not in a fully extended conformation but is nonetheless oriented such that the tpy unit is held remote from the carborane fragment. The approximately planar tpy moiety adopts the expected *trans*,*trans*-conformation [26,27] of the three pyridine rings about the interannular C–C
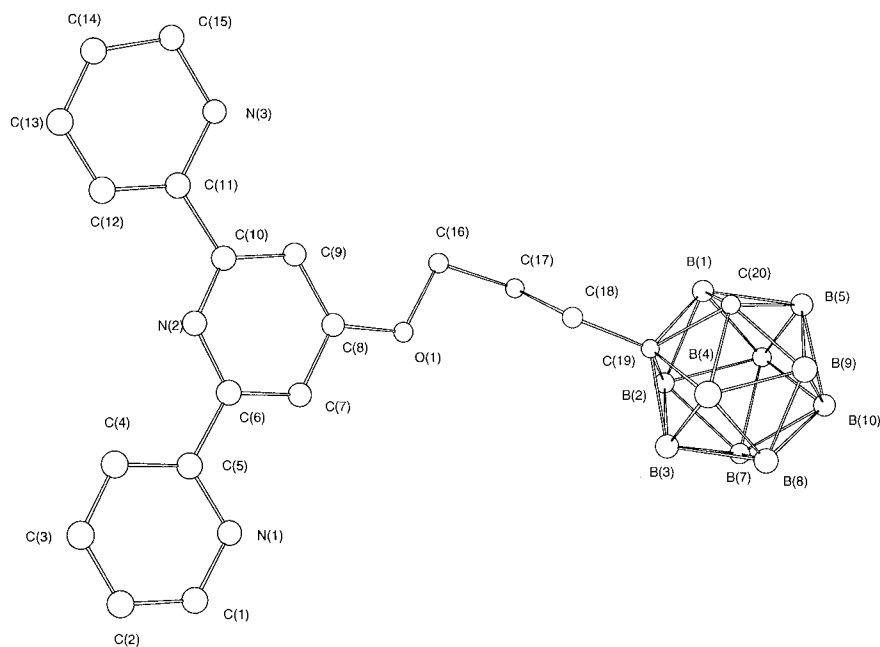

Scheme 2.

Fig. 2. The molecular structure of compound (**4**). Hydrogen atoms are omitted for clarity.

bonds; the torsion angles are given in Table 2. An interesting arrangement of the molecules of (**4**) is observed in the solid-state lattice; the tpy units form stacks with the carbaborane cages residing in channels between the stacks and the crystal lattice is partitioned into distinct tpy and cluster domains. However, the various domains in the lattice interpenetrate to give a complex overall packing arrangement.

Although we had succeeded in preparing a carbaboranyl-functionalised ligand, the low and variable yields of compound (**4**) were not amenable to further investigations of the coordination behaviour of the ligand and so we turned our attention to developing ligand syntheses using the metal-directed substrategy starting from coordinated HOtpy. We have previously reported the preparation of $[Ru(HOtpy)_2][PF_6]_2$ [13]. This complex contains two pendant nucleophilic hydroxy groups which react cleanly with two equivalents of the electrophilic alkyne derivative $HC{\equiv}CCH_2Br$ to yield the ruthenium(II) complex $[Ru(\mathbf{1})_2][PF_6]_2$ in high yield. This complex was fully characterised by the usual means; significant spectroscopic features include the observation of the terminal alkyne proton resonance at δ 3.12 and the methylene group at δ 5.27 in the ^1H NMR spectrum and a resonance at δ 79.1 in the ^{13}C NMR spectrum assigned to the terminal alkynyl carbon atom. The alkyne groups in this complex are expected to show all of their normal reactivity and treatment with decaborane(10) gave a dark-coloured reaction mixture, from which the complex $[Ru(\mathbf{2})_2][PF_6]_2$ was isolated in 27% yield as a red solid after chromatographic separation. The identity of $[Ru(\mathbf{2})_2][PF_6]_2$ was established by elemental analysis, FAB–mass spectrometry and multi-

nuclear NMR spectroscopy. The ^{11}B and ^{13}C NMR spectra were consistent with the presence of equivalent *closo*-$C_2B_{10}H_{11}$ cages and spectroscopic data were in close agreement with those for the carbaboranes discussed above. However, a disadvantage of this synthetic route is the formation of side products arising from additional metal-directed reactions. In this case, the cleavage of the ether chain results in the formation of the compounds $[Ru(\mathbf{2})(HOtpy)][PF_6]_2$ (41% yield) and $[Ru(HOtpy)_2][PF_6]_2$ (6%). The structure of the $[Ru(\mathbf{2})(HOtpy)]^{2+}$ cation is shown in Fig. 1, along with the ring labelling used in the assignments given in the experimental section. The ^1H NMR spectrum of $[Ru(\mathbf{2})(HOtpy)]^{2+}$ is considerably more complicated than those of the homoleptic complexes discussed above. The connectivity within each of the rings of the two non-equivalent tpy ligands was established by COSY spectroscopy and final assignments were made by comparison with the appropriate homoleptic complexes. The most obvious features in the ^1H NMR spectrum of $[Ru(\mathbf{2})(HOtpy)]^{2+}$ are the two singlet resonances assigned to H^{3B} and H^{3D}.

A similar alternative methodology for the synthesis of complexes of (**4**) from $[Ru(HOtpy)_2][PF_6]_2$ in place of HOtpy was also adopted and follows the general strategy shown in Scheme 2. The reaction of $[Ru(HOtpy)_2][PF_6]_2$ with two equivalents of compound (**3**) again resulted in the formation of a dark coloured reaction mixture from which the desired product $[Ru(\mathbf{4})_2][PF_6]_2$ could be isolated as a red solid in 30% yield after chromatography. Characterisation by ^{11}B, ^{13}C and ^1H NMR spectroscopies, elemental analysis and FAB–MS confirmed the identity of the compound and

the presence of two equivalent carbaboranyl-functionalised tpy ligands in the ruthenium(II) complex cation. The NMR spectroscopic data for the carbaborane were in general agreement with those of the free ligand.

In the course of these reactions we noted that the yield of $[Ru(4)_2][PF_6]_2$ was variable and that several other products were formed in significant quantities. The carbaboranyl units in the $[Ru(4)_2]^{2+}$ cation readily undergo boron decapping under the conditions of the synthesis and work-up, and a second product, isolated in 24% yield, was identified as $[Ru(4)(5)][PF_6]$ in which ligand $(5)^-$ contains an anionic *nido*-$[C_2B_9H_{10}]^-$ unit. The structure of the $[Ru(4)(5)]^+$ cation is shown in Fig. 1. The analytical data indicated the presence of a single $[PF_6]^-$ counterion and, assuming that the complex contains ruthenium(II), this is only compatible with the presence of a negatively charged ligand. The ^{11}B NMR spectrum of $[Ru(4)(5)][PF_6]$ contained signals that could be assigned to both a *closo*-C_2B_{10} unit and a *nido*-C_2B_9 moiety. The observation of ^{11}B resonances shifted to higher field (highest field resonance, $\approx \delta -37$) together with *two* carbaboranyl CH resonances, one of which is shifted to higher field with respect to that in $[Ru(4)_2][PF_6]_2$, provide telling evidence for the formation of one anionic *nido* cluster. The FAB mass spectrum of $[Ru(4)(5)][PF_6]$ was also consistent with this formulation exhibiting a highest mass peak at m/z 955 ($\{Ru(4)(5)\}^+$). The remaining material from the reaction of $[Ru(HOtpy)_2][PF_6]_2$ with (3) was strongly absorbed by silica and remained on the baseline during chromatographic purification. NMR spectroscopic examination of material extracted from the silica led us to propose a formulation of $[Ru(5)_2]$ for this compound.

We have investigated the electrochemical behaviour of acetonitrile solutions of the complexes $[Ru(4)_2][PF_6]_2$ and $[Ru(4)(5)][PF_6]$ by cyclic voltammetry. The compound $[Ru(4)_2][PF_6]_2$ exhibits a single reversible Ru(II)/(III) couple at $+0.75$ V vs. Fc/Fc^+ whilst that for $[Ru(4)(5)][PF_6]$ is observed at $+0.74$ V. The similarity in these values and their closeness to that of $[Ru(EtOtpy)_2][PF_6]_2$ (EtOtpy = 4′-ethoxy-2,2′:6′,2″-terpyridine) [13] indicate that the alkoxy-spacer between the tpy and cluster domains prevents there being any meaningful electronic communication between the two. In effect, the complex $[Ru(4)(5)]^{2+}$ exists as a charge localised Zwitterion in which there is no significant interaction between the ruthenium(II) cation and the anionic *nido* cage in the ligand. Although our initial aim had been the development of carbaborane-functionalised ligands, the observation of a range of

metal-directed reactivity prompted us to develop additional ligands in which direct communication between the carbaborane and the tpy was to be expected.

3.3. Direct attachment of the tpy and carbaboranyl domains

Accordingly, the next stage in our investigations was to prepare a ligand in which the heterocyclic and carbaborane domains were directly linked. From our suite of available 4′-substituted tpy ligands, we chose to use 4′-chloro-2,2′:6′,2″-terpyridine (Cltpy) as the precursor to the cluster-functionalised ligand. This ligand is expected to react with nucleophiles at the 4′ site with concomitant loss of chloride. We have noted previously that this process may be accelerated by coordination of the Cltpy to a transition metal centre [22–24]. In principle, reaction of Cltpy with the monoanion of *ortho*-carbaborane should yield a directly linked derivative. However, attempts to prepare monolithiated *ortho*-carbaborane yield mixtures in which dilithiated and non-lithiated compounds predominate (Scheme 3). In his recent developments of the chemistry of 1,2-$C_2B_{10}H_{12}$, Hawthorne has made use of the protecting group Si^tBuMe_2 (TBDMS) and has shown that monolithiation of 1-Si^tBuMe_2-1,2-$C_2B_{10}H_{11}$ is facile and may be used to prepare mono *C*-substituted derivatives [14].

Lithiation of 1-Si^tBuMe_2-1,2-$C_2B_{10}H_{11}$ generated 1-Li-2-Si^tBuMe_2-1,2-$C_2B_{10}H_{10}$ in situ and this was reacted directly with Cltpy in THF. This resulted in the formation of compound (6) as an air stable, colourless solid in 60% yield. The protected carbaborane in ligand (6) is stable in solutions in aprotic solvents, in contrast to the deprotected species (7), as is discussed below. The ^1H, ^{11}B and ^{13}C NMR spectra of solutions of compound (6) were fully consistent with the presence of the 1,2-substituted *closo*-carbaborane cage. The retention of the TBDMS protecting group was confirmed by the observation of resonances at $\delta -0.14$ and 0.88 in the ^1H NMR spectrum. Mass spectrometric and elemental analysis also confirmed the proposed composition.

Compound (6) behaves as a terdentate N,N',N''-donor towards iron(II) and ruthenium(II) and this is illustrated in the formation of the complex cations $[Fe(6)_2]^{2+}$ and $[Ru(tpy)(6)]^{2+}$ under standard reaction conditions. Both the iron(II) and ruthenium(II) complexes have been isolated as the hexafluorophosphate salts. The ^1H, ^{11}B and ^{13}C NMR spectra of CD_3CN solutions of the low-spin, diamagnetic purple complex $[Fe(6)_2][PF_6]_2$ were consistent with the presence of two equivalent *closo*-carbaborane cages. The structure of $[Ru(tpy)(6)]^{2+}$ is shown in Fig. 1, along with the ring nomenclature used for NMR spectroscopic assignments. The ^1H NMR spectrum shows signals in the aromatic region which can be assigned to the two different tpy
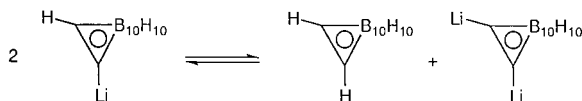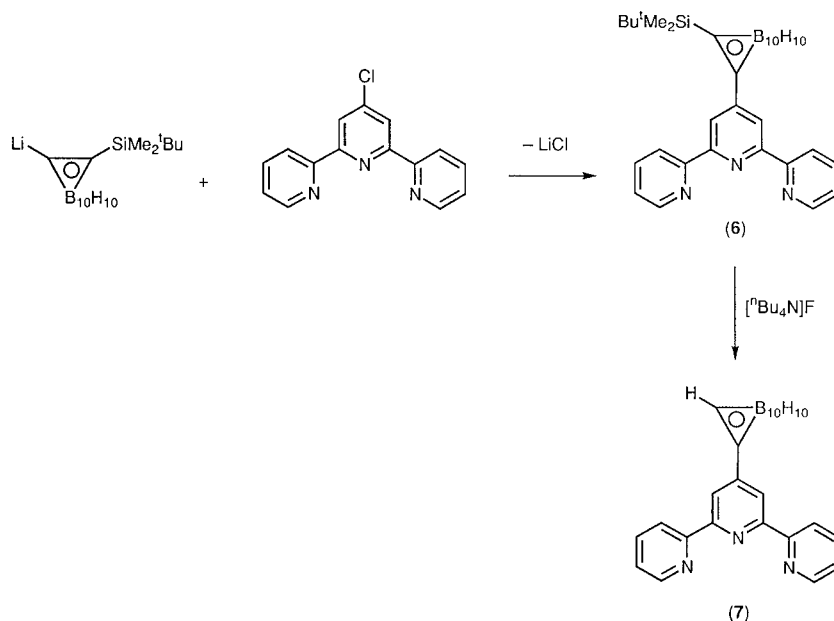
Scheme 3.

environments, whilst the ^{11}B NMR spectrum confirms the presence of a *closo*-C_2B_{10} cage. The mass spectra of both complexes were consistent with their formulations. The electrochemical behaviour of $[Fe(6)_2][PF_6]_2$ and $[Ru(tpy)(6)][PF_6]_2$ has been studied, and in each case reversible metal(II)/(III) redox processes were observed. In the case of $[Fe(6)_2][PF_6]_2$ an iron(II)/(III) process was observed at +0.91 V whilst for $[Ru(tpy)(6)][PF_6]_2$ a process was observed at +1.00 V (all potentials vs. internal Fc/Fc$^+$). These values compare with potentials of +0.74 V and +0.92 V for $[Fe(tpy)_2]^{2+}$ and $[Ru(tpy)_2]^{2+}$, respectively [28,29], and the destabilisation of the M(III) state indicates that the 1-Si^{t}BuMe$_2$-1,2-$C_2B_{10}H_{11}$ substituent is slightly electron withdrawing. Comparison of these data with those described above for the complexes $[Ru(4)_2][PF_6]_2$ and $[Ru(4)(5)][PF_6]_2$ allow an assessment of the effect of having the tpy and carbaboranyl domains directly connected as opposed to being separated by an electronically insulating spacer. Using these data and our previously established linear free energy relationships in systems of this type [13,28,29] it is possible to predict a redox potential for the ruthenium(II)/(III) couple in $[Ru(6)_2][PF_6]_2$ of +1.08 V. Attempts to prepare $[Ru(6)_2][PF_6]_2$ directly from RuCl$_3 \cdot n$H$_2$O always resulted in the formation of mixtures of protected and partially deprotected species.

The silyl protecting group in (6) can be removed under standard conditions, and reaction of (6) with tetrabutylammonium fluoride in THF gave the directly linked deprotected tpy-carbaboranyl ligand (7) (Scheme 4). Analytical, mass spectrometric and NMR spectroscopic data were all in accord with the structure. Once

again, the ^{11}B NMR data fully confirm the presence of an intact *ortho-closo*-carbaboranyl cluster. The deprotection is confirmed by the appearance of the carbaboranyl CH resonance at δ 4.30 in the ^{1}H NMR spectrum. The influence of the spacer may be directly quantified by a comparison of the H$^{3'}$ resonances in compounds (4), (6) and (7). In (4) H$^{3'}$ is observed at δ 7.94 whereas in the directly linked species (6) and (7) H$^{3'}$ is observed at δ 8.76 and 8.52, respectively. This indicates a general deshielding effect of the directly linked cluster and the minor effect of the bulky protecting group. The structure of the deprotected ligand (7), which is related to the previously reported 1-(2-pyridyl)-1,2-$C_2B_{10}H_{11}$ [30], was confirmed by the results of a single crystal X-ray diffraction study.

The molecular structure of (7) is shown in Fig. 3 and selected bond distances and angles are listed in Table 4. The structural parameters for each of the terpyridine and cluster domains are unexceptional [25] and the *closo*-C_2B_{10} cage is ordered; the carbon–carbon distance within the cage is 1.649(1) Å. As expected, the three pyridine rings adopt a *trans,trans* arrangement, and the tpy unit is essentially planar; torsion angles are given in Table 4. The packing of molecules of (7) in the solid-state lattice gives an array in which the tpy units are parallel and the cluster units reside in the channels between them. This is reminiscent of the features we described above for compound (4) but for (7) the array is infinitely ordered (Fig. 4) and interpenetration of parts of the network does not occur.

The deprotection of compound (6) to form (7) is not a straightforward reaction, since loss of the Si^{t}BuMe$_2$ substituent renders the carbaborane cage susceptible to
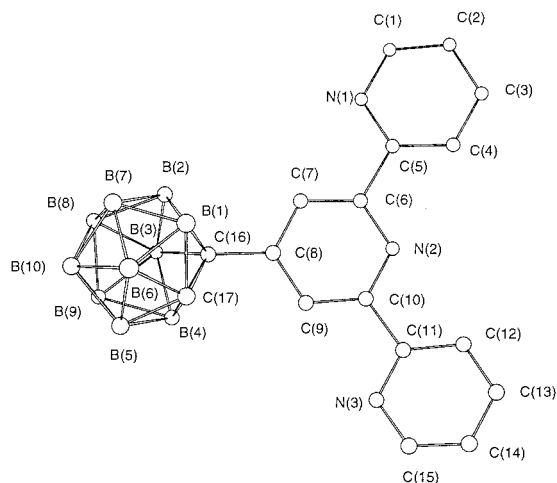

Scheme 4.

Fig. 3. The molecular structure of compound (**7**). Hydrogen atoms are omitted for clarity.

removal of a boron vertex. Thus, in methanol or ethanol solutions, compound (**7**) undergoes a transformation to the Zwitterionic *nido*-derivative (**9**). Scheme 5 shows the decapping process and a possible intermediate in which the *nido*-cage carries two bridging hydrogen atoms. The formation of the Zwitterion (**9**) formally involves the migration of one proton from the cluster to the tpy unit. The low solubility of (**9**) in common organic solvents prevented us from obtaining well re-solved ^1H, ^{13}C or ^{11}B NMR spectra but the TOF mass spectrum showed a parent ion at $m/z = 366$, consistent with the proposed composition.

Complex formation involving ligand (**6**) has been demonstrated by reactions with $[NH_4]_2Fe[SO_4]_2 \cdot 6H_2O$ in methanol or with $[Ru(tpy)Cl_3]$ in methanol in the presence of *N*-ethylmorpholine to yield, after anion exchange, $[Fe(\mathbf{6})_2][PF_6]_2$ and $[Ru(tpy)(\mathbf{6})][PF_6]_2$, respectively. The retention of the *closo*-cluster of (**6**) in the coordinated ligand was confirmed by ^{11}B, ^1H and ^{13}C NMR spectroscopic and mass spectrometric data. In contrast, complex formation with ligand (**7**) was not straightforward. The reaction between $RuCl_3 \cdot 3H_2O$ and (**7**) in ethane-1,2-diol gave a dark red product, for which the TOF–MS exhibited a parent ion at m/z 831. This indicated a neutral product containing two anionic ligands, each a tpy unit bearing a pendant *nido*-$[C_2B_9H_{11}]^-$ group. The ^{11}B NMR spectrum of the product was wholly consistent with this, exhibiting peaks between $\delta -3.40$ and -31.8 with patterns and intensities as expected for this *nido*-cage. The ^1H, ^{13}C and ^{11}B NMR spectra also confirmed the presence of two equivalent ligands. The product is therefore formulated as $[Ru(\mathbf{8})_2]$ where ligand $[(\mathbf{8})]^-$ has the structure shown. The reaction of ligand (**7**) with $[Ru(tpy)Cl_3]$ in methanol in the presence of *N*-ethylmorpholine gave, after anion exchange, $[Ru(tpy)(\mathbf{8})][PF_6]$ in almost quantitative yield. The presence of the *nido*-cluster unit was confirmed by

the appearance in the ^{11}B NMR spectrum of nine equal intensity resonances between $\delta -7.4$ and -34.5. The ^1H NMR spectrum was more complex than that of compound $[Ru(\mathbf{8})_2]$, consistent with the presence of two tpy units in two environments; the spectrum could be assigned by comparison of those of the homoleptic and heteroleptic species. The decapping of the coordinated ligand (**7**) is more facile than that of the free ligand and this observation can be attributed to the enhanced reactivity of the metal coordinated ligand [23].

The electrochemical properties of the complexes $[Fe(\mathbf{6})_2][PF_6]_2$, $[Ru(tpy)(\mathbf{6})][PF_6]_2$, $[Ru(\mathbf{8})_2]$ and $[Ru(tpy)(\mathbf{8})][PF_6]$ have also been investigated. The $[Fe(\mathbf{6})_2]^{2+}$ cation shows a reversible metal-centred one-electron redox process at $+0.91$ V vs. Fc/Fc^+. This compares to the value of $+0.74$ V for $[Fe(tpy)_2]^{2+}$ [28], indicating that the carbaboranyl substituent is slightly electron withdrawing. Similarly, $[Ru(tpy)(\mathbf{6})]^{2+}$ exhibits a reversible one-electron process at $+1.00$ V compared to $+0.92$ V for $[Ru(tpy)_2]^{2+}$ [28]. Reversible redox processes for $[Ru(\mathbf{8})_2]$ and $[Ru(tpy)(\mathbf{8})]^+$ at $+0.80$ V and $+0.86$ V reveal that the *nido*-cage is also
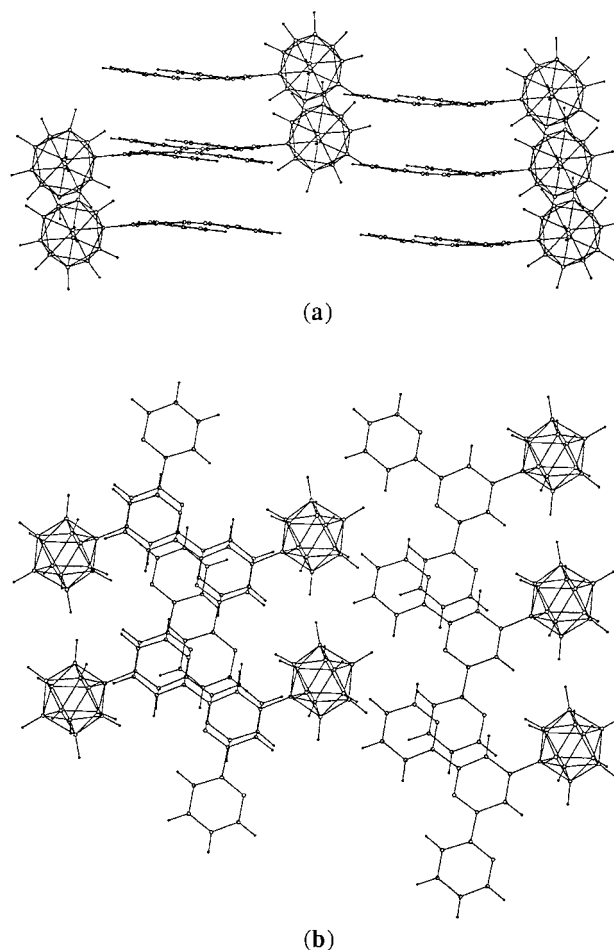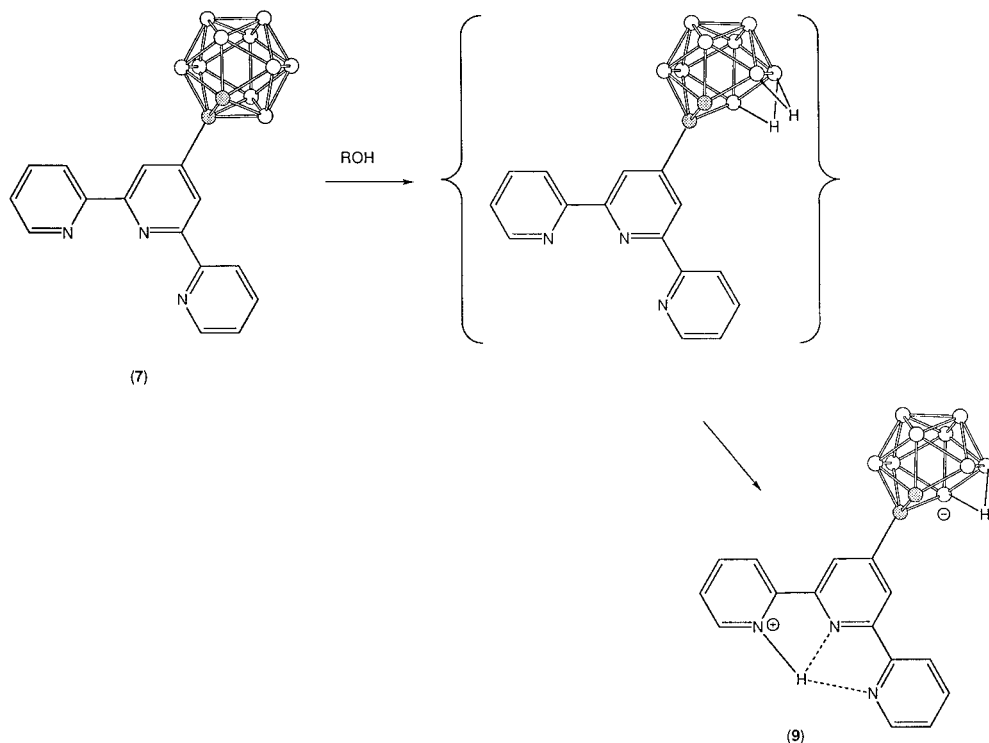

(**a**)

(**b**)

Fig. 4. Two views (related by rotation) of the packing of molecules of (**7**) in the solid state showing the stacking of the tpy units and the discrete tpy and cluster domains.

Scheme 5.

slightly electron withdrawing. These data all indicate that directly linking the carbaborane unit to the tpy metal-binding domain results in significant electronic communication between the metal and the cluster.

4. Conclusions

In conclusion, we have shown that carbaboranyl functionalised tpy ligands may be prepared using conventional 'organic' reactions or by using the metal-directed reactivity of coordinated Xtpy ligands. We are currently investigating the incorporation of these ligands into metallodendrimers.

Acknowledgements

References

[1] E.C. Constable, Chem. Ind. (1994) 56.
[2] E.C. Constable, P. Harverson, M. Oberholzer, Chem. Commun. (1996) 1821.
[3] D. Armspach, M. Cattalini, E.C. Constable, C.E. Housecroft, D. Phillips, Chem. Commun. (1996) 1823.
[4] E.C. Constable, P. Harverson, Chem. Commun. (1996) 33.
[5] E.C. Constable, P. Harverson, Inorg. Chim. Acta. 252 (1996) 9.
[6] E.C. Constable, Chem. Commun. (1997) in press.
[7] E.C. Constable, C.E. Housecroft, in: J.D. Wuest (Ed.), Self-assembly in Synthetic Chemistry, Kluwer, Dordrecht, 1997, in press.
[8] D. Armspach, E.C. Constable, C.E. Housecroft, M. Neuburger, M. Zehnder, Supramol. Chem. 7 (1996) 97.
[9] D. Armspach, E.C. Constable, C.E. Housecroft, M. Neuburger, M. Zehnder, New J. Chem. 20 (1996) 331.
[10] D. Armspach, E.C. Constable, F. Diederich, C.E. Housecroft, J.-F. Nierengarten, Chem. Commun. (1996) 2009.
[11] E.C. Constable, R.-A. Fallahpour, J. Chem. Soc., Dalton Trans. (1996) 2389.
[12] E.C. Constable, M.D. Ward, J. Chem. Soc., Dalton Trans. (1990) 1405.
[13] E.C. Constable, A.M.W. Cargill Thompson, D.A. Tocher, New J. Chem. (1992) 855.
[14] F.A. Gomez, M.F. Hawthorne, J. Org. Chem. 57 (1992) 1384.
[15] A. Altomare, G. Cascarano, G. Giacovazzo, A. Guagliardi, M.C. Burla, G. Polidori, M. Camalli, SIR92, J. Appl. Crystallogr. 27 (1994) 435.
[16] D. Watkin, CRYSTALS, Issue 9, Chemical Crystallography Laboratory, Oxford, 1990.
[17] J.A. Ibers, W.C. Hamilton (Eds.), International Tables for X-ray Crystallography, vol. IV, Kynoch Press, Birmingham, 1974, Tables 2.2B and 2.3.1.
[18] E.C. Constable, A.M.W. Cargill Thompson, D.A. Tocher, in: V. Balzani, L. De Cola (Eds.), Supramolecular Chemistry, Kluwer, Dordrecht, 1992, p. 219.
[19] E.C. Constable, in: L. Fabbrizzi, A. Poggi (Eds.), Transition Metals in Supramolecular Chemistry, Kluwer, Dordrecht, 1994, p. 81.
[20] T. Onak, Polyhedral Carbaboranes in: vol. ed. C.E. Housecroft, editors-in-chief E.W. Abel, F.G.A. Stone, G. Wilkinson, Comprehensive Organometallic Chemistry II, vol. 1, Pergamon, Oxford, 1995, p. 217.

[21] C.E. Housecroft, Carbaboranes, including their Metal Complexes in: E.W. Abel (Ed.), Specialist Periodical Reports: Organometallic Chemistry, The Royal Society of Chemistry, London, 1996, p. 26, and previous reviews in this series.

[22] E.C. Constable, Inorg. Chim. Acta 82 (1984) 53.

[23] E.C. Constable, Metals and Ligand Reactivity — An Introduction to the Organic Chemistry of Metal Complexes, VCH, Weinheim, 1995.

[24] E.C. Constable, T.A. Leese, Inorg. Chim. Acta 146 (1988) 55.

[25] R.A. Beaudet, in: J.F. Liebman, A. Greenberg, R.E. Williams (Eds.), Advances in Boron and the Boranes, VCH, New York, 1988, p. 417.

[26] E.C. Constable, F.K. Khan, V.E. Marquez, P.R. Raithby, Acta Crystallogr. Sect. C 48 (1992) 932.

[27] C.A. Bessel, R.F. See, et al., J. Chem. Soc., Dalton Trans. (1992) 3223.

[28] E.C. Constable, A.M.W. Cargill Thompson, J. Chem. Soc., Dalton Trans. (1994) 1409.

[29] E.C. Constable, A.M.W. Cargill Thompson, J. Chem. Soc., Dalton Trans. (1992) 2947.

[30] R. Coult, M.A. Fox, W.R. Gill, Herbertson, J.A.H. MacBride, K. Wade, J. Organometal. Chem. 462 (1993) 19.